Kathmandu University
Journal of Science, Engineering and Technology

Bello *et. al.*, Vol. 12, No. I, June, 2016, pp 63-79.

ORIGINAL RESEARCH ARTICLE OPEN ACCESS

PHYSICAL PROPERTIES OF COCONUT SHELL NANOPARTICLES

[1,2]Bello S. A.[*], [2]Agunsoye J. O., [2,3]Adebisi J. A., [2,4]Kolawole F. O., [2]Hassan S. B.
[1]Department of Materials Science and Engineering, Kwara State University, Malete, Nigeria
[2]Department of Metallurgical and Materials Engineering, University of Lagos, Nigeria
[3]Department of Metallurgical and Materials Engineering, University of Ilorin, Nigeria
[4]Department of Metallurgical and Materials Engineering, Federal University, Oye-Ekiti, Nigeria

[*]Corresponding author's e-mail: adekunle_b@yahoo.com
Received 31 March, 2016; Revised 4 June, 2016

ABSTRACT

Physical properties such as apparent density, bulk density, compressibility index and particle sizes of carbonized and uncarbonized coconut shell nanoparticles produced through top down approach have been studied. Percentage composition of the coconut fruit was determined using five different coconut fruit samples. Results revealed that coir occupies the highest percentage; coconut shells account for 15 % while the flesh and liquid occupy 30 % of the whole coconut fruit. The apparent densities of the uncarbonized and carbonized coconut shell nanoparticles obtained at 70 hours of milling are 0.65 g/cm^3 and 0.61 g/cm^3 respectively. Their respective compressibility indices and average particle sizes are 46.4 % and 69.7 %; 50.01 nm and 14.29 nm. The difference in the particle sizes of the carbonized and uncarbonized coconut shell nanoparticles can be linked with reduction in the moisture content and volatiles of the carbonized coconut shell nanoparticles due to carbonization process. The reduction in the moisture and volatiles results in the enhanced hardness and brittleness of the carbonized coconut shells which facilitate their breakage during the course of milling than that of the uncarbonized coconut shells.

Keywords: Carbonized coconut shell, Carbonization, Compressibility index, Physical property, Percentage composition.

INTRODUCTION

Carbon particles/fibres possess outstanding properties. They have high specific modulus which outweighs that of the steel. Their thermal and electrical conductivities are excellent in comparison with those of competing materials such as ceramics and polymers [1]. The carbon has numerous applications which includes fuel for heating, adsorbent medium for purification and fillers for composite fabrication [2-4]. They are produced from either polyacrylonitrile (PAN), coal, petroleum, pitch or trees. PAN, coal, petroleum and pitch are all non-renewable resources. Exploitation of petroleum and coal are also associable with environmental impacts and carbon materials produced from these sources are highly expensive. Carbon production from trees involves falling and burning of trees, which can lead to deforestation; a hazardous effect that can lead to global warming. Therefore sourcing of carbon material from renewable resources such as agro products is highly imperative [5].

Agricultural products release a huge amount of materials such as coconut, palm kernel, ground nut and walnut shells which are potential resources for carbon production. These materials are cheap, easily available and renewable. Their usage for carbon production does not affect food supply for human

Bello *et. al.*, Vol. 12, No. I, June, 2016, pp 63-79.

consumption. Annually, 12,280 hectares of land are cultivated for coconut trees, from which 64.3 billion nuts are harvested, an equivalent mass of 62.8 billion tons. Coconut shell occupies 15 % of a total weight of a coconut fruit which means an approximate 9 million tons of the coconut shells are discarded globally every year. Structurally, coconut shell contains mainly cellulose, hemicellulose, lignin and moisture which are potential sources of carbon [6].

Thermochemical process leading to conversion of carbonaceous materials to fixed carbon is called carbonization. During the process, carbonaceous materials are heated in an inert environment in a closed container (crucible) to a high temperature to dry and burn off the volatiles in the material. Different temperatures have been used for carbonizing coconut shells ranging between 600 and 1200°C [7, 8]. The carbon obtained from the process is least dusty and much harder when compared with those obtained from other agricultural products [9].

In this present work, an attempt has been made to study the properties both of carbonized and uncarbonized coconut shell nanoparticles. Although many studies have reported production of coconut shell micro particles as a reinforcement for matrix composite production [10-17], the detail synthesis and characterization of the carbonized coconut shell in respect of particle sizes with milling duration is very scarce.

MATERIALS AND METHODS

Uncarbonized and carbonized coconut shell nanoparticles are the major materials used in this study. The equipment used includes SNH tumbler ball mill, model A 50….43, heat resistant electric furnace, Veleta transmission electron microscope and ASPEX 3020 scanning electron microscope. Initially, percentage composition each of the components of the coconut fruit was determined using five different coconut fruits. Mass of the coconut fruits was determined using Pioneer weighing scale of 0.001 readability and recorded as M_o. The measurement was repeated after removal of coconut coir, liquid and flesh. The mass in each case was designated as M_1, M_2 and M_3 respectively as shown in Plate 1a. Uncarbonized coconut shell nanoparticles were produced using ball milling techniques. They were milled for maximum of 70 hours, particles taken at 16, 46 and 70 hours were characterized in accordance with [3, 18-20]. However, synthesis of carbonized coconut shell nanoparticles started with crushing of the dried coconut shell. Then, the crushed coconut shells were heated to 1000˚C at an average heating rate of 6˚C/minutes in a controlled atmosphere of muffle furnace using a closed steel container as a crucible, and held at this temperature for 2 hours after which, they were cooled to room temperature. Plate 1b presents the carbonized coconut shells.

a

Kathmandu University
Journal of Science, Engineering and Technology

Plate 1: (a) Disassembling of coconut fruits for mass measurement (b) Carbonized coconut shells

The carbonized coconut shells were pulverized and sized using a disc grinder and set of sieves arranged in ascending order of grain fineness. The sizing was carried out in accordance with [12, 21, 22]. The carbonized coconut shell powders collected in a pan below 56 µm sized sieve were ball milled for 70 hours at 10 charge ratios using the tumbler ball mill with ceramic balls of different sizes in accordance with [3, 19]. The procedure for the synthesis both of carbonized and uncarbonized coconut shell nanoparticles is presented in Figure 1. Different samples taken at 16, 46 and 70 hours were analyzed using SEM, TEM, XRD and UV-Vis spectrophotometer. The unsettled bulk, the tapped apparent density and compressibility index both of carbonized and uncarbonized coconut shell nanoparticles were determined in accordance with method A of [23].

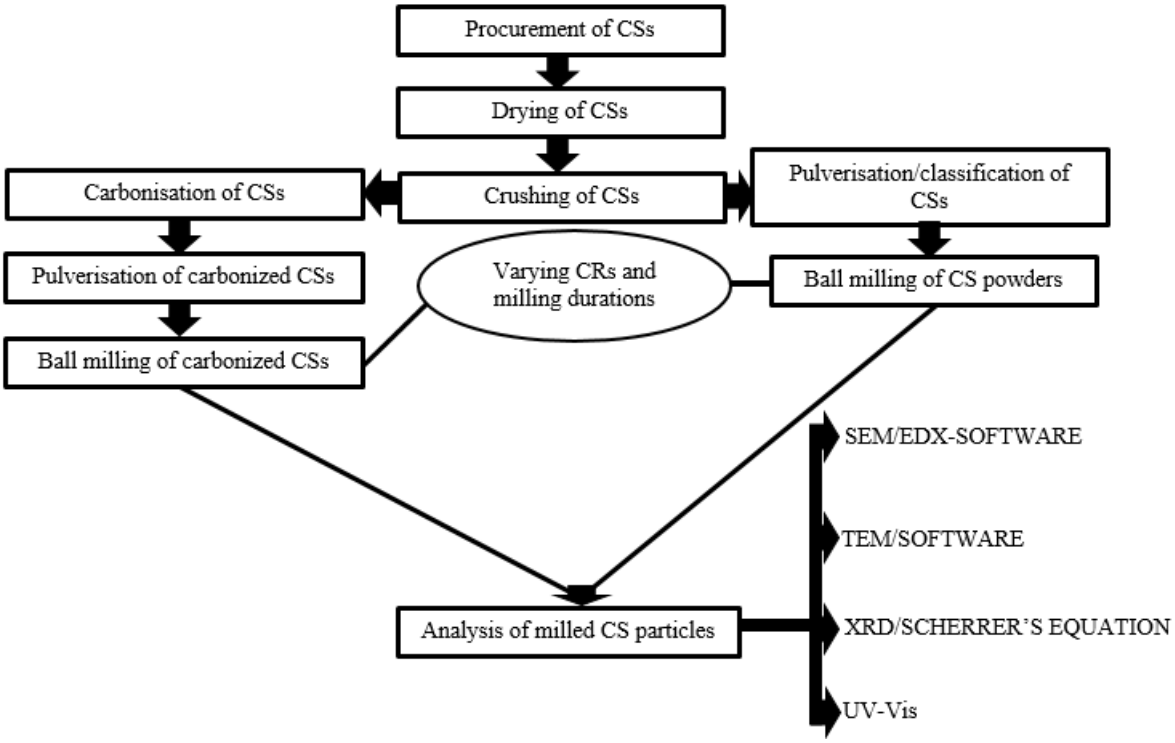

Figure 1: Chart for the synthesis of Coconut Shell Nanoparticles

Kathmandu University
Journal of Science, Engineering and Technology

Bello *et. al.*, Vol. 12, No. I, June, 2016, pp 63-79.

RESULTS AND DISCUSSIONS

Percentage compositions of coconut shells

Analysis of coconut fruits revealed that the coconut fruit contains outer, middle and inner layers [3, 19]. The outer layer contains coir which occupies 54.38±0.7 % of the coconut fruit. The middle layer is the coconut shell. This layer occupies 15.18±2.4 % while the inner layer contains both edible flesh and drinkable liquid. The flesh and liquid account for 22.31±2.4 % and 8.11±2.6 % respectively, equivalent to 30.42±5 % of the whole coconut fruit (see Table 1).

Table 1: Average composition of Coconut Shells

Coconut fruits	M_o (g)	M_1 (g)	M_2 (g)	Mass of coconut shell M_3 (g)	Mass of coir M_o-M_1 (g)	Mass of liquid M_1-M_2 (g)	Mass of flesh M_2-M_3 (g)	Percentage composition			
								Coconut shells	Coir	Liquid	Flesh
1	960	440	380	170	520	60	210	17.7	54.17	6.25	21.88
2	1090	500	380	180	590	120	200	16.42	54.13	11.01	18.35
3	880	400	300	100	480	100	200	11.36	54.55	11.36	22.73
4	810	360	320	110	450	40	210	13.58	55.56	4.94	25.93
5	860	400	340	145	460	60	195	16.86	53.49	6.98	22.67
Total	4600			705	2500	380	1015	75.92	271.88	40.54	111.5
Average composition (%)								15.18±2.4	54.38±0.7	8.11±2.6	22.31±2.4

XRD of coconut shell nanoparticles

Figure 2a-c present the XRD profiles of carbonized coconut shell nanoparticles obtained at 16, 46 and 70 hours respectively. In Figure 2a major peaks of carbonized coconut shell nanoparticles (CCNPs) indicated C, SiO_2 and Fe at respective diffraction angles (2Θ) of 30.89, 51.23° and 72.45. The inter-planar spacing is 4.2, 3.36 and 2.07 Å. The diffractogram in Figure 2b shows SiO_2, 2H; C and FeNi at 24.37, 31.07 and 52.36° respectively at the major peaks. Their respective inter-planar spacing is 4.24, 3.34 and 2.03*Å*. At 70 hours, phases of CCNPs are SiO_2, C, Fe_3O_4 and Fe (Figure 2c). These occurred at diffraction angles and inter-planar spacing of 24.2, 30.87, 51.26 and 52.23° and 4.1, 3.36, 2.07 and 2.03 Å respectively. Fe compounds could be associated with chemical interaction between Fe and carbonized coconut shells

Kathmandu University
Journal of Science, Engineering and Technology

during the course of milling. Presence of Fe may be due to pilling of inner surface of the steel container (used as the crucible) during the process of carbonization. The increased particle surface energy built-up during milling process enhanced chemical interaction between Fe and CCNPs, leading to formation of the Fe compounds and others. The difference in the inter-planar spacing is an indication of differences in the CCNPs' orientation which could be linked with severe plastic deformation due to ball impacts.

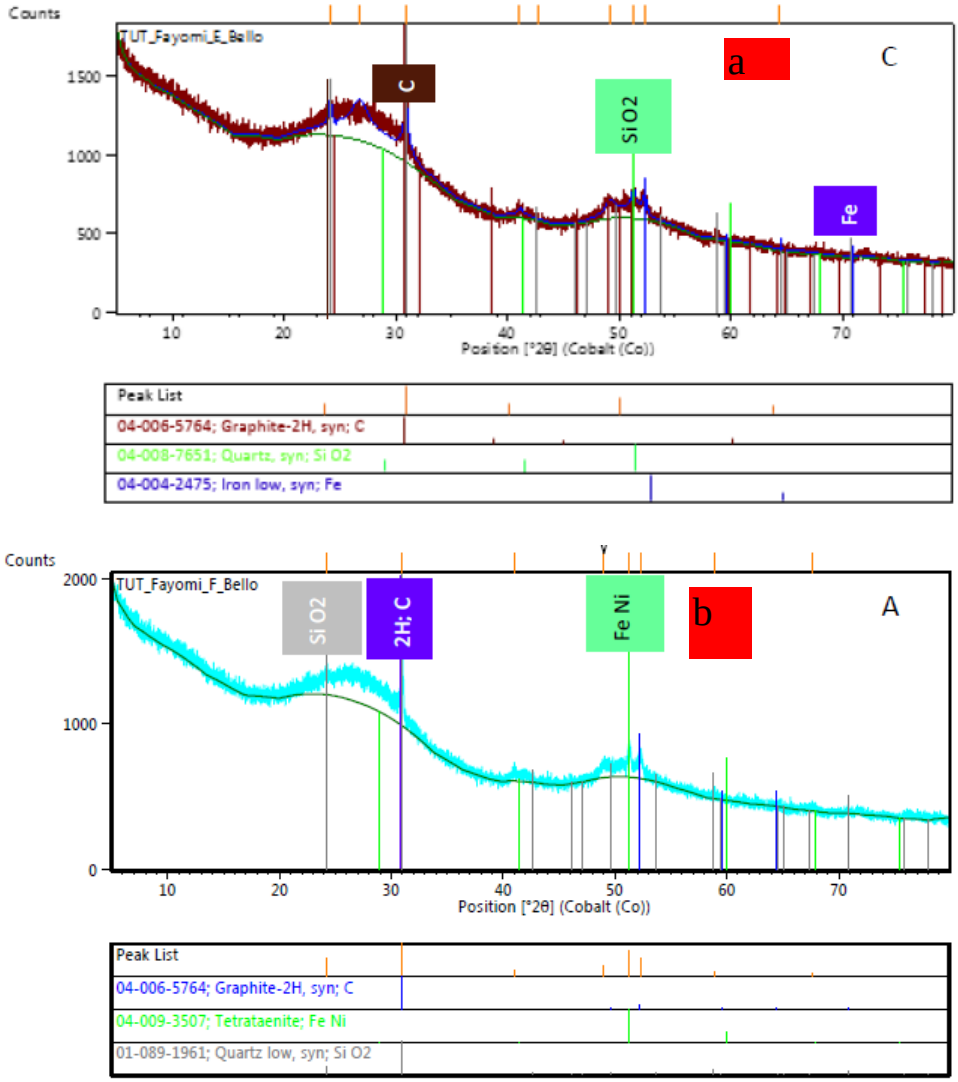

Kathmandu University
Journal of Science, Engineering and Technology

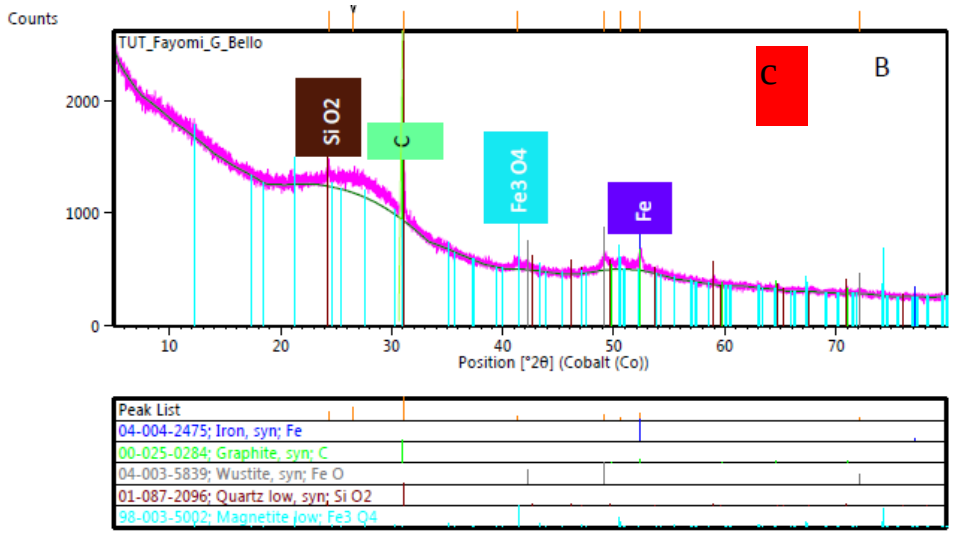

Figure 2: XRD profiles of CCNPs obtained at (a) 16, (b) 46 and (c) 70 hours

SEM of CCNPs

The microstructure in Plate 2a shows the carbonized coconut shells in networks of polygonal layers having pores of different sizes and shapes. The pores made the carbonized CSs brittle and facilitated their breakage during the milling process. Energy dispersive X-ray (EDX) spectrograph reveals C as the major element. Percentage mass difference estimation using equation 1 indicated that 78.68 % of the charged coconut shells accounted for burnt-off substances during the carbonization process. This agrees with literature [8].

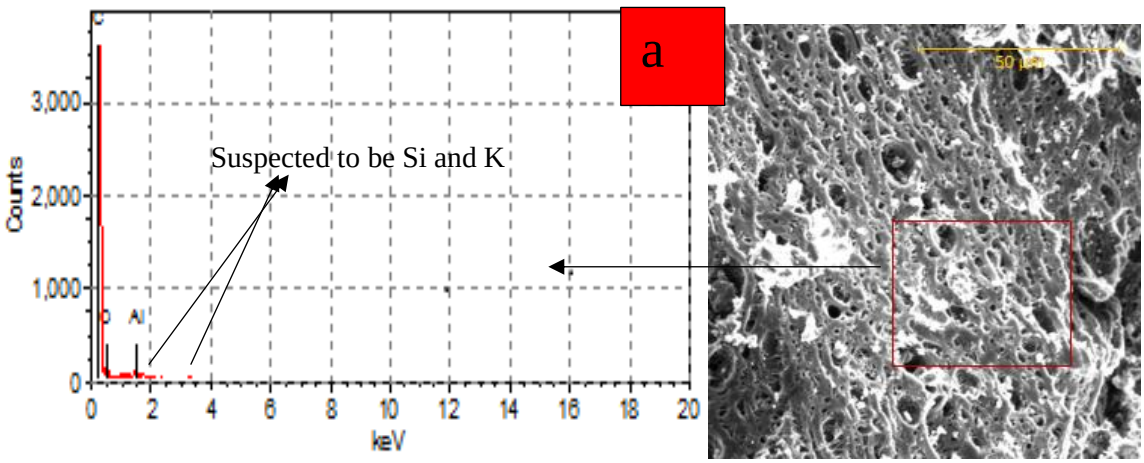

Kathmandu University
Journal of Science, Engineering and Technology

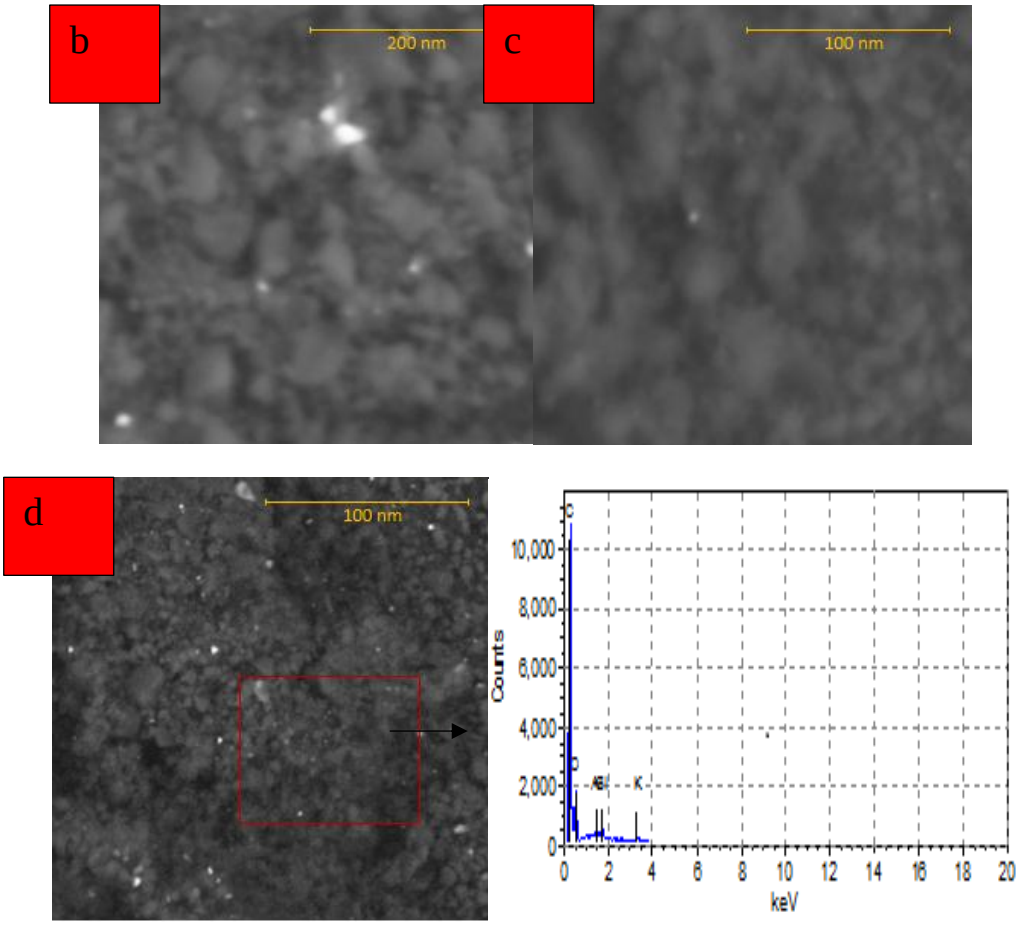

Plate 2: SEM/EDX of (a) Carbonised CSs, (b-d) CCNPs at 16 , 46, 70 hours

$$\%mass = \frac{mass\ before\ carbonisation - mass\ after\ carbonisation}{mass\ after\ carbonisation} x\ 100 \qquad 1$$

Microstructures of CCNPs in Plate 2b-d show particles having different morphologies. CCNPs obtained at 16 hours of milling existed in different shapes which can be classified spherical, ellipsoidal and polygonal (Plate 2b). This could be attributable to brittle fracture of the carbonized CSs during the course of milling.

As the ball fell on the particles, they mounted different form of breaking forces such as impact, attrition, shear and compression on the particles. Once the force overcame the cohesive forces within the particles, the particles became shattered in brittle manner due to inner/intra layer pores into smaller sizes characterized with different shapes. For instance, when carbonized coconut shell particles were under compression, the large intra/inter layer pores attempted to close up. During this process, cleavage occurred within the particles leading to their fracture. As the milling duration increased from 16 to 46 hours, CCNPs were appearing smaller with all their shapes approached spherical shapes though their sizes were different

Kathmandu University
Journal of Science, Engineering and Technology

Bello *et. al.*, Vol. 12, No. I, June, 2016, pp 63-79.

(see Plate 2c). This is due to continual breakages of the particles due to ball impacts. Plate 2d depicts microstructure of extremely fine CCNPs obtained at 70 hours. The degree of particle miniaturization due to increased milling duration can be clearly seen by comparing the microstructures in Plate 2b-d. Despite that the resolution in Plate 2d is the same as that in Plate 2c, as less than that in Plate 2b, the CCNPs in Plate 2d appeared much smaller and the microstructure is much brighter than their counterparts in Plate 2b-c. EDX spectrograph in Plate 2d revealed the presence of C, O, Al, Si and K. This agrees with elemental composition of the unmilled carbonized CSs except Si and K. Absence of Si and K in EDX spectrograph in Plate 2a could be due to the fact that their count scores were so small that they could not be detectable as an individual element. The increment in the carbon count score from about 3800 to 11000 is an indication of an increment in the number of CCNP fragments produced from the initial carbonized CS powders during the process of milling. This led to an increment in the number of CCNPs which was accompanied with reduction in their sizes.

TEM of CCNPs

TEM images of the CCNPs at 16, 46 and 70 hours of milling were displayed in Plate 3a-c. It was observed that CCNPs appeared in different forms at varying milling durations. They form central big clusters of different geometries, around which there are many discrete smaller particles. They assume different shapes at an angle of tilt during TEM analysis. As the milling duration increased, the big central CCNP cluster became smaller due to breakage. Number of discrete particles appeared greater. This indicated a continual surface wear and breakage of the cluster due to attrition by grinding media as the milling duration increased, leading to a change in the morphology and orientation of the particles.

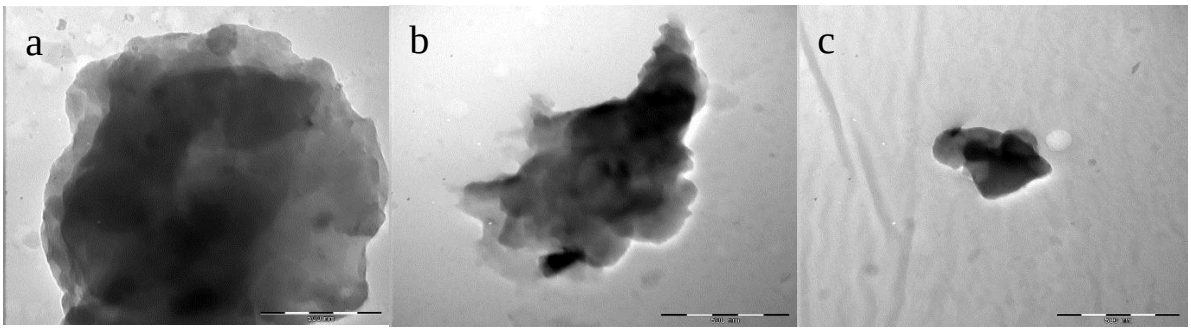

Plate 3: TEM images of CCNPs obtained at (a) 16, (b) 46 and (c) 70 hours

Optical properties of CCNPs

Figure 3a-c presents the optical properties of CCNPs obtained at 16, 46 and 70 hours of milling. In these figures, amount of light absorbed by particles during analysis was plotted against the wavelength of the radiation. The curve appearance and peak varied from one milling duration to another indicating different behavior of the CCNPs during analysis. As the milling duration increased, there was an increase in the light absorbed by the CCNPs from 1.0 at 16 hours of milling to 3.28 at 70 hours of milling indicating that black colors of CCNPs became more darkened. This contradicted the decrease in the absorbance observed with UCSNPs in [3]. The increase in the absorbance could be attributable to a decrease in the diameter of

Kathmandu University
Journal of Science, Engineering and Technology

inter/intra layer pores (mesopores) as the milling progressed. As the particle breakage occurred, each CCNP fragment from the carbonized coconut shell powders has smaller diameter pores. The decrease in the pore diameter continued as long as the new fragments or cells were formed due to breakage of the initial particles.

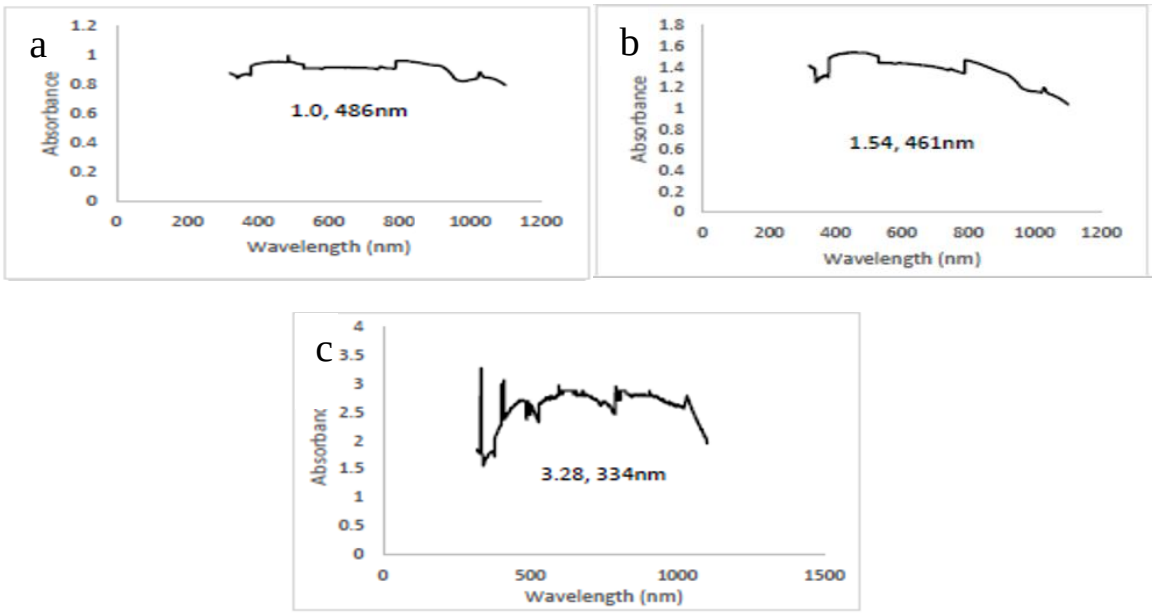

Figure 3: UV-Vis spectra of CCNPs

The decrease in pore sizes reduced the chances of UV-Vis radiation to travel through pores within the CCNPs during optical analysis thereby enhancing the movement of radiation through the actual layers of the CCNPs. Since large amount of radiations interacted with the layers in the smaller particles, amount of radiation absorbed tended to be higher than that in the large CCNPs which possessed large mesopores. Since the mesopore sizes were decreased, the amount of air trapped into the CCNPs was reducing, thereby intensifying the dark color of the CCNPs (see Figure 4).

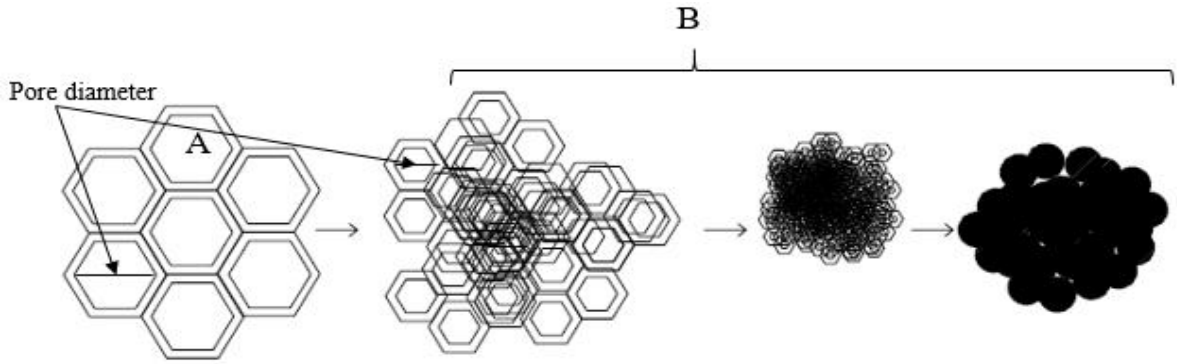

Figure 4: Carbonized coconut shell (A) before and (B) during milling

Kathmandu University
Journal of Science, Engineering and Technology

Bulk and apparent densities

Result of density and compressibility index determination revealed that the unsettled bulk density, the tapped apparent density and compressibility index of the uncarbonized coconut shell nanoparticles are 0.34 g/cm^3, 0.65 g/cm^3 and 46.4% respectively while those of uncarbonized coconut shell micro particles (< 56 µm) are 0.64 g/cm^3, 0.88 g/cm^3 and 37.4 % respectively. The carbonized coconut shell nanoparticles have bulk density of 0.45 g/cm^3, the tapped apparent density of 0.61 g/cm^3 and compressibility index of 69.7 % respectively while those of carbonized coconut shell micro particles are 0.57 g/cm^3, 0.7 g/cm^3 and 20.8 % respectively. The difference in the density parameters and compressibility index of carbonized and uncarbonized coconut shell particles is attributable to variation in the chemical compositions of the particles and their sizes.

Sizes of coconut shell nanoparticles

Imaging particle sizes of uncarbonized coconut shell nanoparticles obtained from SEM aided with software are presented in Plate 4a-c. Tomography in Plate 4 showed that the average particles sizes of uncarbonized coconut shell nanoparticles at 16, 46 and 70 hours of milling are 119.2 nm, 72.1 nm and 49.85 nm respectively. Figure 5 presents the uncarbonized coconut shell nanoparticle sizes and their distributions at different milling durations. The difference in the curve geometry reveals the decrease in the particle sizes as the milling duration increased. The value on the horizontal axis corresponding to the maximum peak of each curve presents the average particle size of the uncarbonized coconut shell particles at respective milling durations.

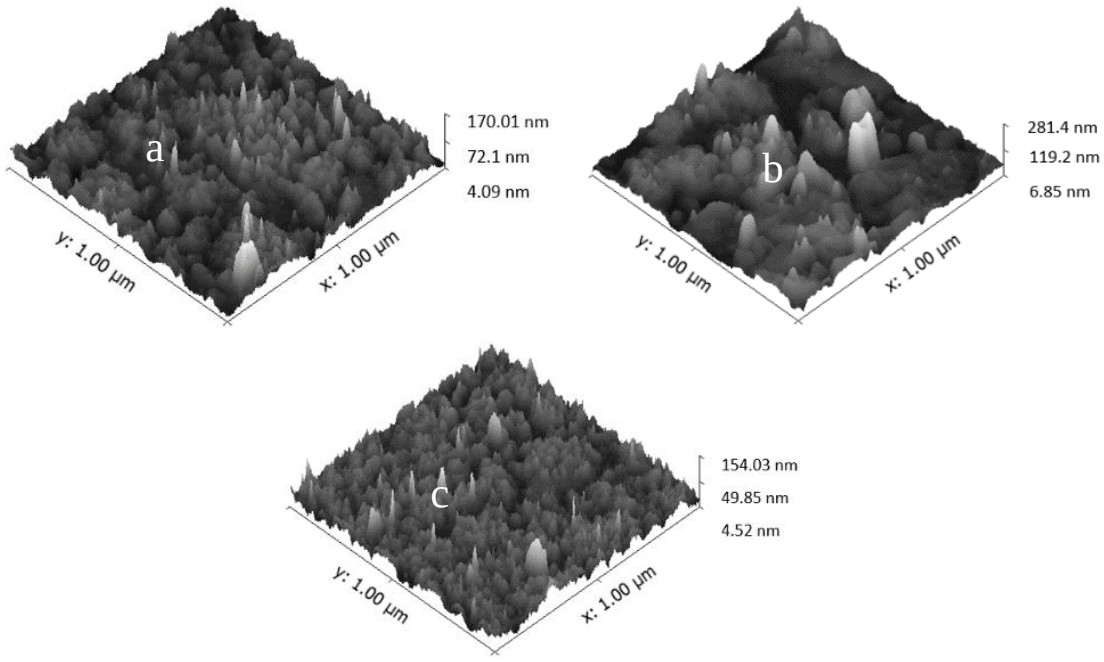

Plate 4: Tomography of UCSNPs at (A) 16, (B) 46, (C) 70 hours

Kathmandu University
Journal of Science, Engineering and Technology

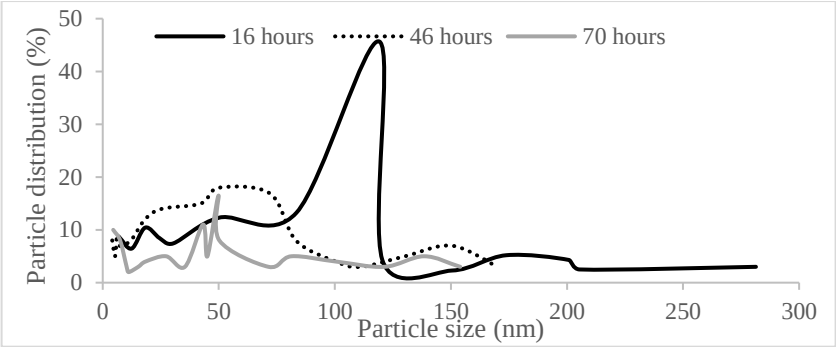

Figure 5: UCSNP size distribution at constant milling duration

Crystallites sizes of CCNPs determined from XRD aided with Scherrer's equation reveal that the minimum, maximum and averages sizes at 16 hours of milling are 14.90, 74.29 and 31.37 nm respectively. At 46 hours, the sizes are 3.36, 41.72 and 20.17 nm while the sizes at 70 hours are 0.55, 24.58 and 12.47 nm respectively. SEM/Gwyddion tomography in Plate 5 shows the maximum and minimum sizes with structural features of CCNPs. Their respective average sizes are 50.01, 31.76 and 14.29 nm. Figure 6 displays the CCNP sizes and the distribution. The crystallite and pictorial sizes obtained from XRD/Scherrer's equation and SEM/Gyweddion were compared in Figure 7. It was observed that crystallite sizes are slightly smaller than pictorial sizes. This can be linked with the fact that the XRD presented the crystallite sizes while the image size obtained from the SEM depicts the actual particle sizes. However, a particle can contain one or more crystals.

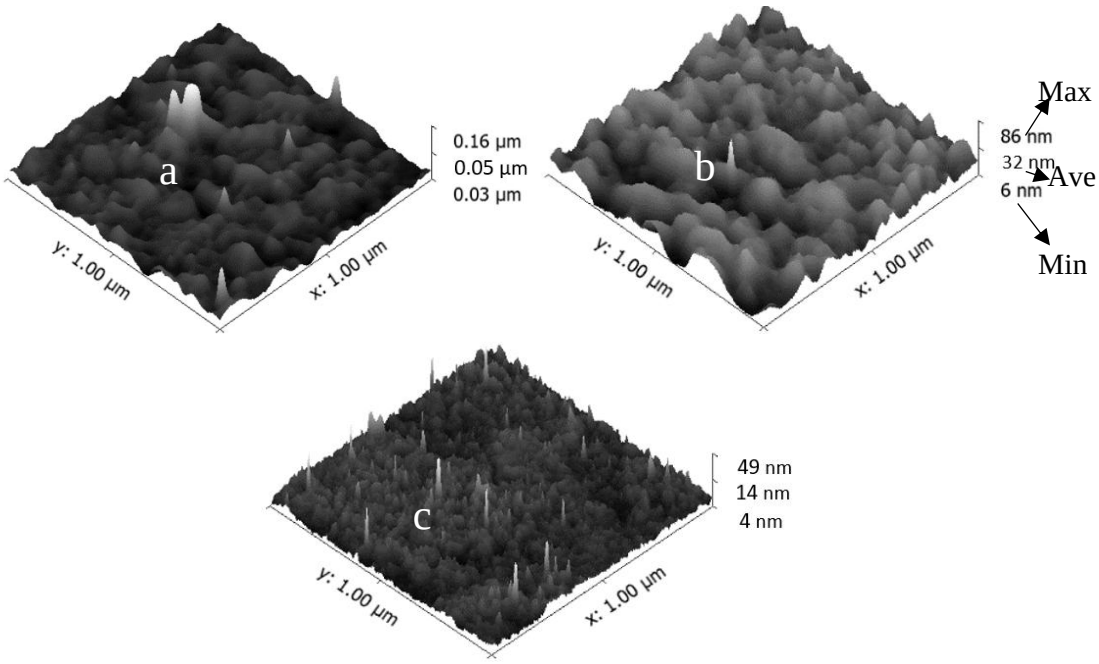

Plate 5: Tomography of CCNPs at (a) 16, (b) 46 (c) 70 hours

Kathmandu University
Journal of Science, Engineering and Technology

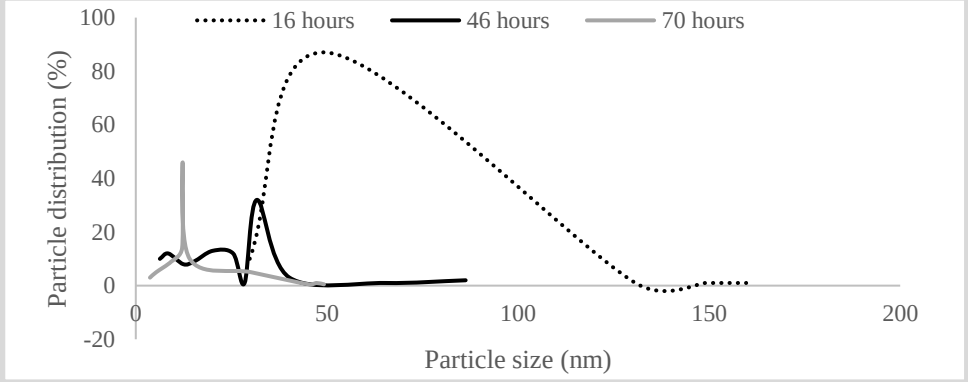

Figure 6: Percentage distribution of CCNPs

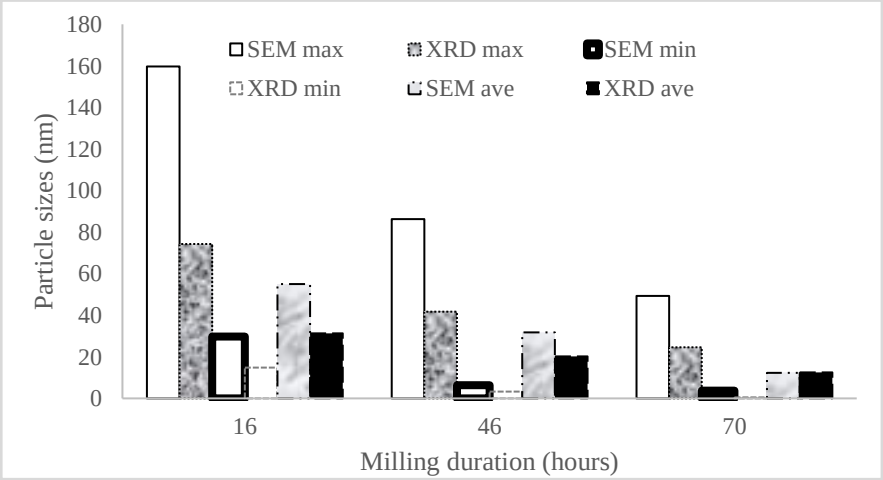

Figure 7: Particle sizes with milling duration

Relationship between CCNP sizes, milling duration and light absorbance was studied by drawing the graph of optical properties in Figure 8-9. Figure 8 indicated an increase in the maximum absorbance as the milling duration increased. At the same time, there was a decrease in the wavelength at which the maximum absorbance occurred. A positive relation between wavelength at maximum absorbance and particle sizes, deduced from Figure 9 indicated a decrease in the particle sizes with a decrease in the maximum absorbance wavelength as the milling progressed to 70 hours.

Kathmandu University
Journal of Science, Engineering and Technology

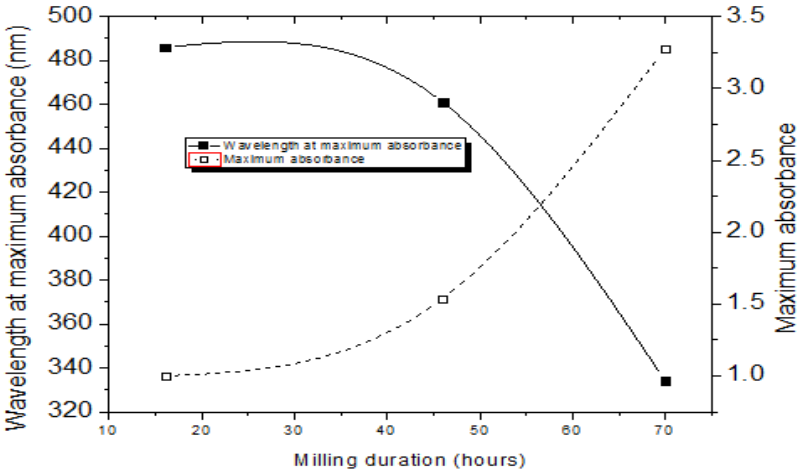

Figure 8: Optical properties with milling duration

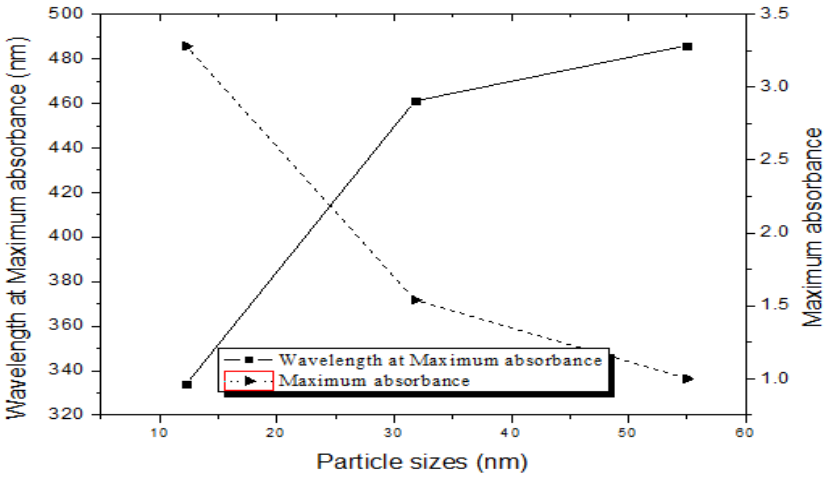

Figure 9: Optical properties with particle sizes

In the case of maximum absorbance, the opposite trend is the case i.e. the absorbance increased with a decrease in the CCNP sizes. Since for every formation of CCNP fragments from initial carbonized coconut shell powders, there was a decrease in the initial size. The inverse relation holds between the sizes of the CCNPs and their numbers. If d and n represent the CCNP sizes and number, therefore equation 2 holds.

$$n\,\alpha\,\frac{1}{d}\;;\; n=\frac{k}{d}, \qquad 2$$

K is a constant depending on milling parameters.

Kathmandu University
Journal of Science, Engineering and Technology

At 16, 46 and 70 hours, number of CCNPs are expressed in Table 2. Since equal amount of each sample of CCNPs was dissolved in 2 ml of solvent during the sample preparation for UV-Vis analysis, therefore, concentration [c] of the solution per ml of solvent could be expressed as

$$[c] = \frac{n}{2} \qquad 3$$

Table 2: CCNP properties

Milling durations (hours)	d (nm)	N	[c] (n/ml)
16	55.01	0.018179k	0.009089k
46	31.76	0.031486k	0.015743k
70	12.29	0.081367k	0.040683k

A plot of absorbance with concentration of CCNPs in Figure 10 indicated a positive linear relation as the milling progressed to 70 hours. This agrees with Beer-Lambert relation [24].

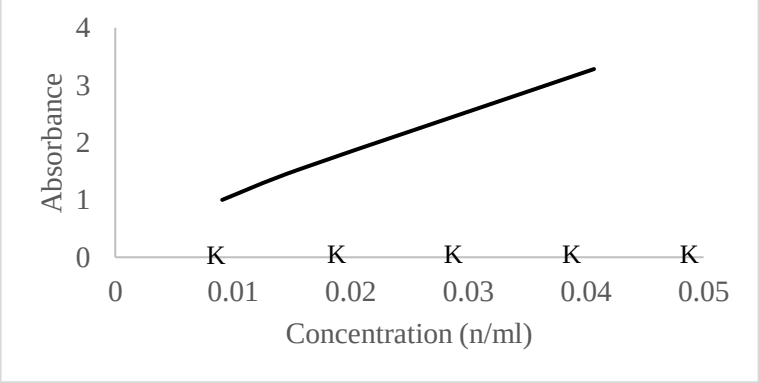

Figure 10: Absorbance with concentration

By comparing the particle sizes of carbonized and uncarbonized coconut shell nanoparticles using Figure 11, it was observed that the particle size of CCNPs (50.01 nm) obtained at 16 hour of milling is very close to that (49.85 nm) of UCSNPs obtained at 70 hours (see Figure 11). This behavior can be linked with the brittleness enhancement in respect of CCNPs due to carbonization.

Kathmandu University
Journal of Science, Engineering and Technology

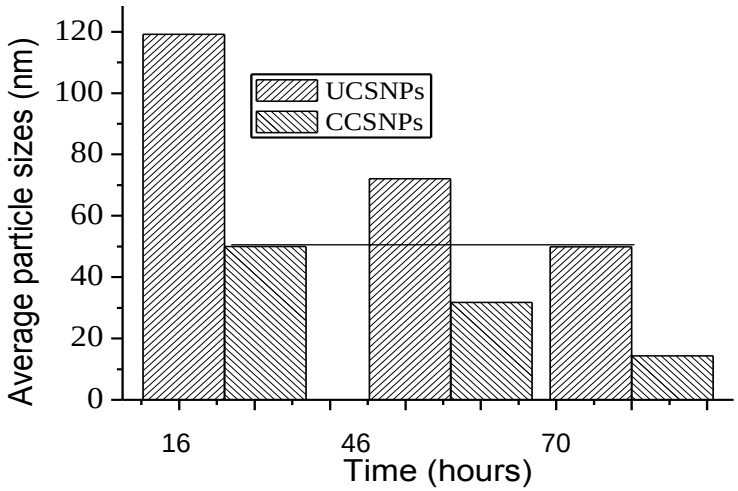

Figure 11: Average particle sizes of UCSNPs and CCNPs

CONCLUSION

Upon the experimentation and results of investigation of this study, the following conclusions can be inferred:

[1] Carbonized coconut shell nanoparticles have been synthesized using a ball milling technique.
[2] Variation of the carbonized coconut shell nanoparticle sizes agrees with results of the previous study.
[3] The variation in the compressibility indices, bulk and apparent densities of the carbonized and uncarbonized coconut shell nanoparticles can be linked with difference in their chemical compositions and sizes.
[4] The brittleness imparted to coconut shells due to carbonization enhanced their breakage during the course of milling.
[5] The decrease in the sizes of mesopores within the carbonized coconut shell nanoparticle could be responsible for the increment in the light absorbance as the milling duration increased.

ACKNOWLEDGEMENT

Authors wish to express their appreciation to members of staff of Department of Ceramics, Federal Industrial Institute of Research Oshodi, Nigeria; Department of Metallurgical and Materials Engineering, University of Lagos; Department of Materials Science and Engineering, Kwara State University, Malete; Mrs. A. A. Bello and A. O. Bello-Raji for their enormous support in making this work a reality. Thank you all.

REFERENCES

[1] Peters S T, HANDBOOK OF COMPOSITES, S.T. Peters, England: Springer Science Business Media Donlrecht, (1998) 2: 1135.

[2] Daud W M A W & Ali W S W, Comparison of pore Development of Activated Carbon produced Palm Kernel and Coconut shells, Bioresource Technology, (2004) 93: 63-69.

[3] Bello S A, Agunsoye J O & Hassan S B, Synthesis of Coconut Shell Nanoparticles Via A Top Down Approach: Assessment of Milling Duration on The Particle Sizes and Morphologies of Coconut Shell Nanoparticles, *Materials Letters*, (2015) 159: 514-519.

[4] Abiko H, Furuse M & Takano T, Reduction of Adsorption Capacity of Coconut Shell Activated Carbon for Organic Vapors Due to Moisture Contents, *Industrial Health*, (2010) 48: 427-437.

[5] Bello S A, Development and Characterization of Epoxy/Al (1050)/Coconut shell Particulate Hybrid Nanocomposites, Department of Metallurgical and Materials Engineering, University of Lagos: Nigeria, (2015) i-iii, 132.

[6] Romulo N A, *Market and Trade of Coconut Products*, Asian and Pacific Coconut Community: Thailand, (2013) 1-122.

[7] Chanap R, Study of Mechanical and Flexural Properties of Coconut Shell Ash Reinforced Epoxy Composites, Department of Mechanical Engineering, *National Institute of Technology Rourkela*, (2012) 41.

[8] Gimba C E & Turoti M, Optimum Condition for Carbonisation of Coconut shells, *Scientia Africana*, (2008) 7(4): 12-21.

[9] Li W *et. al.*, Effects of carbonization temperatures on characteristics of porosity in coconut shell chars and activated carbons derived from carbonized coconut shell chars, *Industrial Crops and Products*, (2008) 28(2): 190-198.

[10] Agunsoye J O *et. al.*, Recycled Polypropylene Reinforced Coconut Shell Composite: Surface Treatment Morphological, Mechanical and Thermal Studies, *International Journal of Composite Materials*, (2014) 4(3): 168-178.

[11] Agunsoye J O *et. al.*, The Effects of Cocos Nucifera (Coconut Shell) on the Mechanical and Tribological Properties of Recycled Waste Aluminium Can Composites, *Tribology in Industry*, (2014) 36(2): 155-162.

[12] Bello S A, Raheem I A & Raji N K, Study of tensile properties, fractography and morphology of aluminium (1xxx)/coconut shell micro particle composites, *Journal of King Saud University - Engineering Sciences* (2015).

[13] Bhaskar J & Singh V K, Water Absorption and Compressive Properties of Coconut Shell Particle Reinforced-Epoxy Composite, *J. Mater. Environ. Sci.*, (2013) 4(1): 113-118.

[14] Bledzki A K, Mamun M M & Volk J, Barley husk and coconut shell reinforced polypropylene composites: The effect of fibre physical, chemical and surface properties, *Composites Science and Technology*, (2010) 70(5): 840-846.

[15] Sapuan S M, Harimi M & Maleque M A, Mechanical Properties of Epoxy/Coconut shell Filler Particle Composites, *The Arabian Journal for Science and Engineering*, (2003) 28(2B): 171-181.

[16] Sarki J *et. al.*, Potential of using coconut shell particle fillers in eco-composite materials, *Journal of Alloys and Compounds*, (2011) 509(5): 2381-2385.

[17] Singh V K & Bhaskar J, Physical and Mechanical Properteis of Coconut Shell Particles Reinforced Epoxy Composites, *J. Mater. Environ. Sci.*, (2013) 4(2): 227-232.

[18] Bello S A *et. al.*, Characterization of Coconut Shell Nanoparticles using Electron Microscopes, *Unilag Journal of Medicine, Science and Technology* (2016). (In press)

[19] Bello S A *et. al.*, Synthesis of Uncarbonised Coconut Shell Nanoparticles: Characterisation and Particle Size Determination, *Tribology in Industry*, (2015) 37(2): 257-263.

[20] Hassan S B, Agunsoye J O & Bello S A, Production of Carbonized Coconut shell Nanoparticles Using Ball Milling, *Toronto'2016 AES-ATEMA International Conference*, Canada (2016).

[21] Agunsoye J O *et. al.*, Assessment of mechanical and wear properties of epoxy based hybrid composites, *Advances in Production Engineering & Management*, (2016) 11(1): 5-14.

[22] Hassan S B, Agunsoye J O & Bello S A, Ball Milling Synthesis of Al (1050) Particles: Morphological Study and Particle Size Determination, *Industrial Engineering Letters*, (2015) 5(11): 22-27.

[23] S.3.6. Bulk Density and Tapped Density of Powders Final Text for Addition to the International Pharmacopoeia, Bulk-Tapped-Densityqas11_450FINAL_MODIFIEDMARCH2012.pdf., World Health Organisation, (2012) 1-6.

[24] Kaminski C F, *Analytical Chemistry, 8 lectures, Michaelmas Term 2013*, Chemical Engineering Section (2013).